

AD-A059 650

PENNSYLVANIA STATE UNIV UNIVERSITY PARK APPLIED RESE--ETC F/6 20/13  
AN ANALYTICAL STUDY OF HEAT TRANSFER IN A TWO-PHASE, SOLID-LIQU--ETC(U)  
JUN 78 M W NANSTEEL, C H WOLGEMUTH

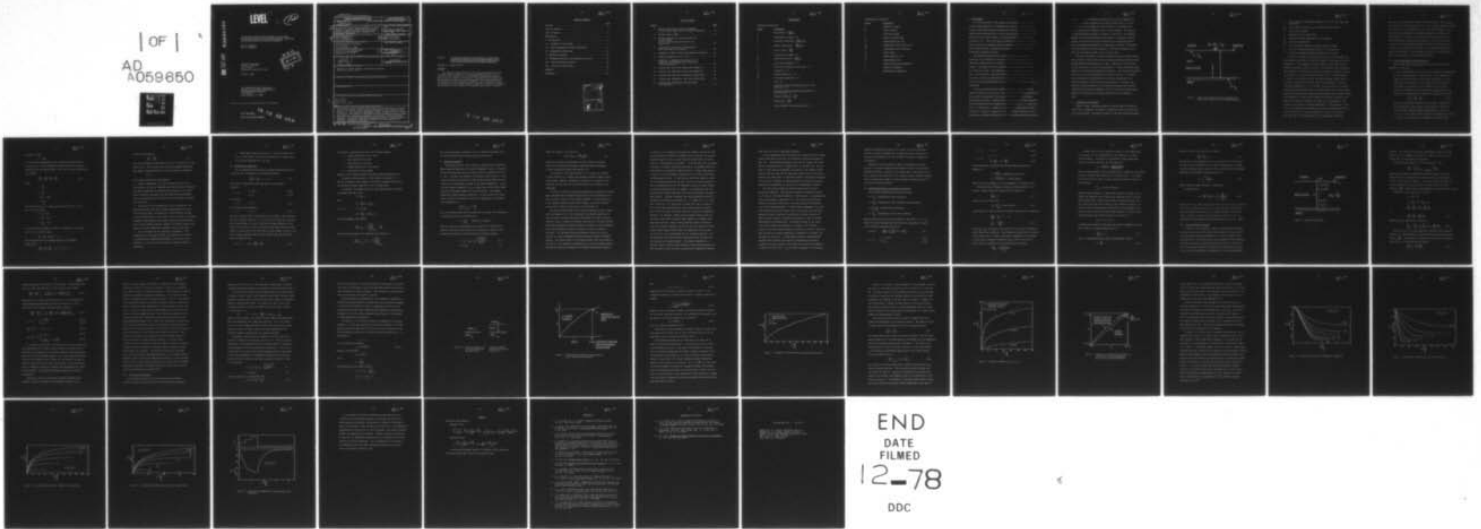
UNCLASSIFIED

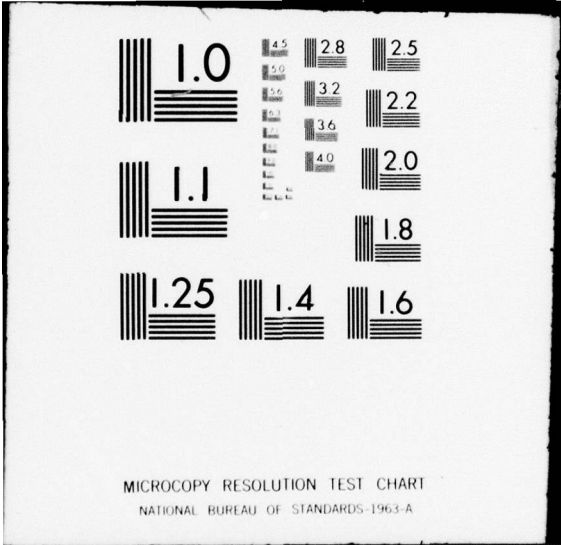
TM-78-178

N00017-73-C-1418

NL

| OF |  
AD  
A059650





AD A059650

DDC FILE COPY

LEVEL

12

AN ANALYTICAL STUDY OF HEAT TRANSFER IN A TWO-PHASE  
SOLID-LIQUID MEDIUM WITH TIME VARYING BOUNDARY CONDITIONS  
AT BOTH THE MOVING AND STATIONARY BOUNDARIES

Mark W. Nansteel  
Carl H. Wolgemuth

Technical Memorandum  
File No. TM 78-175  
June 7, 1978  
Contract No. N00017-73-C-1418

Copy No. 6

DDC  
OCT 11 1978  
F

The Pennsylvania State University  
Institute for Science and Engineering  
APPLIED RESEARCH LABORATORY  
P. O. BOX 30  
State College, PA 16801

Approved for public release distribution unlimited.

NAVY DEPARTMENT  
NAVAL SEA SYSTEMS COMMAND

78 09 29 030

UNCLASSIFIED

SECURITY CLASSIFICATION OF THIS PAGE (When Data Entered)

REPORT DOCUMENTATION PAGE		READ INSTRUCTIONS BEFORE COMPLETING FORM
1. REPORT NUMBER <b>14</b> TM-78-175	2. GOVT ACCESSION NO.	3. RECIPIENT'S CATALOG NUMBER
6. TITLE (and Subtitle) AN ANALYTICAL STUDY OF HEAT TRANSFER IN A TWO-PHASE, SOLID-LIQUID MEDIUM WITH TIME VARYING BOUNDARY CONDITIONS AT BOTH THE MOVING AND STATIONARY BOUNDARIES	5. TYPE OF REPORT & PERIOD COVERED 9 Final Rept.	
	6. PERFORMING ORG. REPORT NUMBER	
7. AUTHOR(s) 10 Mark W. Nansteel Carl H. Wolgemuth	8. CONTRACT OR GRANT NUMBER(s) 15 N00017-73-C-1418	
9. PERFORMING ORGANIZATION NAME AND ADDRESS Applied Research Laboratory P. O. Box 30 State College, PA 16801	10. PROGRAM ELEMENT, PROJECT, TASK AREA & WORK UNIT NUMBERS	
11. CONTROLLING OFFICE NAME AND ADDRESS Naval Sea Systems Command Washington, DC 20360	12. REPORT DATE 11 17 June 1978	
	13. NUMBER OF PAGES 45	
14. MONITORING AGENCY NAME & ADDRESS (If different from Controlling Office) 12 48p.	15. SECURITY CLASS. (of this report) Unclassified	
	15a. DECLASSIFICATION/DOWNGRADING SCHEDULE	
16. DISTRIBUTION STATEMENT (of this Report) Approved for public release; distribution unlimited. Per NAVSEA Sept. 6, 1978.		
17. DISTRIBUTION STATEMENT (of the abstract entered in Block 20, if different from Report)		
18. SUPPLEMENTARY NOTES		
19. KEY WORDS (Continue on reverse side if necessary and identify by block number) heat transfer phase change solid-liquid system		
20. ABSTRACT (Continue on reverse side if necessary and identify by block number) The following report provides a brief outline and description of the steps taken in formulating a simple mathematical model for the analysis of heat transfer in a pure substance undergoing a change in phase (solid to liquid or vice-versa). The problem is approached from the differential point of view and eventually the governing equations are solved by a finite difference technique. The results show fairly conclusively that the present method of analysis is capable of predicting the behavior of such a system to a reasonably high degree of accuracy.		

391007

B



Subject: An Analytical Study of Heat Transfer in a Two-Phase,  
Solid-Liquid Medium With Time Varying Boundary Condi-  
tions at Both the Moving and Stationary Boundaries

References: Pages 44 and 45.

ABSTRACT

The following report provides a brief outline and description of the steps taken in formulating a simple mathematical model for the analysis of heat transfer in a pure substance undergoing a change in phase (solid to liquid or vice-versa). The problem is approached from the differential point of view and eventually the governing equations are solved by a finite difference technique. The results show fairly conclusively that the present method of analysis is capable of predicting the behavior of such a system to a reasonably high degree of accuracy.

78 09 29 030

TABLE OF CONTENTS

	Page
Abstract. . . . .	1
Table of Contents . . . . .	2
List of Figures . . . . .	3
Nomenclature. . . . .	4
I. Introduction . . . . .	6
II. Statement of the Problem . . . . .	7
III. Basic Assumptions in Model Formulation. . . . .	10
IV. Mathematical Formulation . . . . .	13
V. Methods of Analysis . . . . .	15
VI. Nondimensionalization and Asymptotic Solution. . . . .	19
VII. Finite Difference Solution. . . . .	22
VIII. Results and Conclusions. . . . .	26
Appendix. . . . .	43
References. . . . .	44

ACCESSION for	
NTIS	Write Section <input checked="" type="checkbox"/>
DDC	B.H.F. Section <input type="checkbox"/>
UNANNOUNCED	<input type="checkbox"/>
U.S. DEPARTMENT OF ENERGY	
BY	
DISTRIBUTION/AVAILABILITY CODES	
Dist	SPECIAL
A	

LIST OF FIGURES

<u>Figure</u>		<u>Page</u>
1.	Sketch Illustrating the Basic Arrangement of Solid Layer, Rigid Wall, and Liquid Freestream. . . . .	8
2.	Variable Nodal System. . . . .	23
3.	Initial Condition for the Stefan Solution, No Solid Layer. Initial Condition Specified in Part IV, $S=S_0$ at $t=0$ . . . . .	29
4.	Illustration of Method for Comparing the Exact and Numerical Solutions. . . . .	30
5.	Comparison of Exact (Stefan) and Numerical Solutions. . . . .	32
6.	Asymptotic Behavior for $S_t \rightarrow 0$ . . . . .	34
7.	Comparison of Temperature Gradients at the Interface, Actual Temperature Profile and Linear Approximation . . . . .	35
8.	Constant Heat Flux, Wall Temperature Stepped Up. . . . .	37
9.	Constant Wall Temperature, Heat Flux Stepped Up. . . . .	38
10.	Constant Heat Flux, Wall Temperature Stepped Down. . . . .	39
11.	Constant Wall Temperature, Heat Flux Stepped Down. . . . .	40
12.	Constant Wall Temperature, Step-Wise Heat Flux Variation . . . . .	41

NOMENCLATURE

## Dimensional Quantities:

<u>Symbol</u>	<u>Description</u>
c	heat capacity - $\frac{\text{Btu}}{\text{lbm-}^\circ\text{F}}$
d	characteristic length - ft
h	convective conductance - $\frac{\text{Btu}}{\text{hr-ft}^2\text{-}^\circ\text{F}}$
k	thermal conductivity - $\frac{\text{Btu}}{\text{hr-ft-}^\circ\text{F}}$
ℓ	heat of fusion - $\frac{\text{Btu}}{\text{lbm}}$
L	characteristic length - ft
q <sub>c</sub> <sup>''</sup>	convective heat flux - $\frac{\text{Btu}}{\text{hr-ft}^2}$
S	solid layer thickness - ft
S <sub>0</sub>	solid layer thickness at zero time - ft
T	temperature - °F
T <sub>m</sub>	melting temperature - °F
T <sub>∞</sub>	freestream temperature - °F
t	time - hr
x	position coordinate measured parallel to the solid wall - ft
y	position coordinate measured perpendicular to the solid wall - ft
α	thermal diffusivity - $\frac{\text{ft}^2}{\text{hr}}$
ρ	mass density - $\frac{\text{lbm}}{\text{ft}^3}$
τ	time coordinate for Stefan solution - hr



Nondimensional Quantities:

<u>Symbol</u>	<u>Description</u>
b	numerical constant
Fo	Fourier modulus
n	nodal point index
N	denotes interface node
q*	dimensionless heat flux
q <sub>i</sub> *	dimensionless heat flux for t<0
S*	dimensionless solid thickness
St	Stefan number
St <sub>i</sub>	Stefan number for t<0
t*	dimensionless time
δ	symbol denoting small magnitude
η	similarity parameter
θ	dimensionless temperature

## I. INTRODUCTION

The study presented in this paper was initiated in order to gain a better understanding of the phenomena occurring in a two-phase (solid-liquid) system under transient temperature conditions. The general phase change problem considered here is one of great practical interest in the areas of nuclear reactor safety, the solidification of metal castings, cryogenics, etc.. Due to the mutual presence of two phases, this problem defies solution by techniques commonly employed in problems of conduction heat transfer because the region in which the solution is sought is continuously changing with time.

The immediate application of the present analysis concerns the prediction of the behavior of the solid product layer adjacent to the tube walls (heated side) in a Rankine cycle steam boiler-liquid metal reactor. The amount and rate of deposition of solid product is sought as a function of time. The fundamental goal or objective in this study then, is to formulate a simplified mathematical model which may be used to predict the rate of solidification or melting in a two-phase system such as the one described above for a given set of initial and boundary conditions.

The basic problem of heat transfer with phase change has avoided general solution for a long time. The analytical difficulties encountered can be mainly attributed to the nonlinear character of the governing differential equations. Numerous particular solutions have been presented in the literature (see for example, Carslaw and Jaeger (1), J. Stefan (2), and I. G. Portnov (3) ). However, in general, the application of these solutions is limited to systems with special boundary conditions of the type which are seldom encountered in real-world melting and solidification



phenomena. Numerous approximate methods have also been suggested including variational techniques and integral methods similar to those developed by Th. von Karman for the calculation of two-dimensional laminar and turbulent boundary layers in fluid dynamics. The accuracy of these approximate methods is in general a function of the immediate problem but they are nevertheless very powerful. Relatively accurate results can be secured with these methods with the additional benefit that the mathematical complexity is significantly reduced in comparison to the more general solution techniques. The various methods of solution will be elaborated upon later on in this paper.

The brief discussion of solution methods given above already implies that in order to obtain results for the general melting and solidification problem numerical techniques must be used. Therefore, the major effort in this study will be toward the development of a finite difference approximation for the governing differential equations. The resulting difference equations will be solved numerically by digital computer. The results will be presented in dimensionless form so that the effects of the various parameters can be more easily interpreted. An integral type analysis is being developed at this time which possesses some favorable characteristics even when compared to the full finite difference method, however, the details of the integral method will not be discussed here.

## II. Statement of the Problem

Figure 1 shows a two-phase system of solid and liquid in which the solid layer is bounded on one side by a rigid wall and on the other side by the liquid phase. The symbols in Figure 1 have the following meanings.

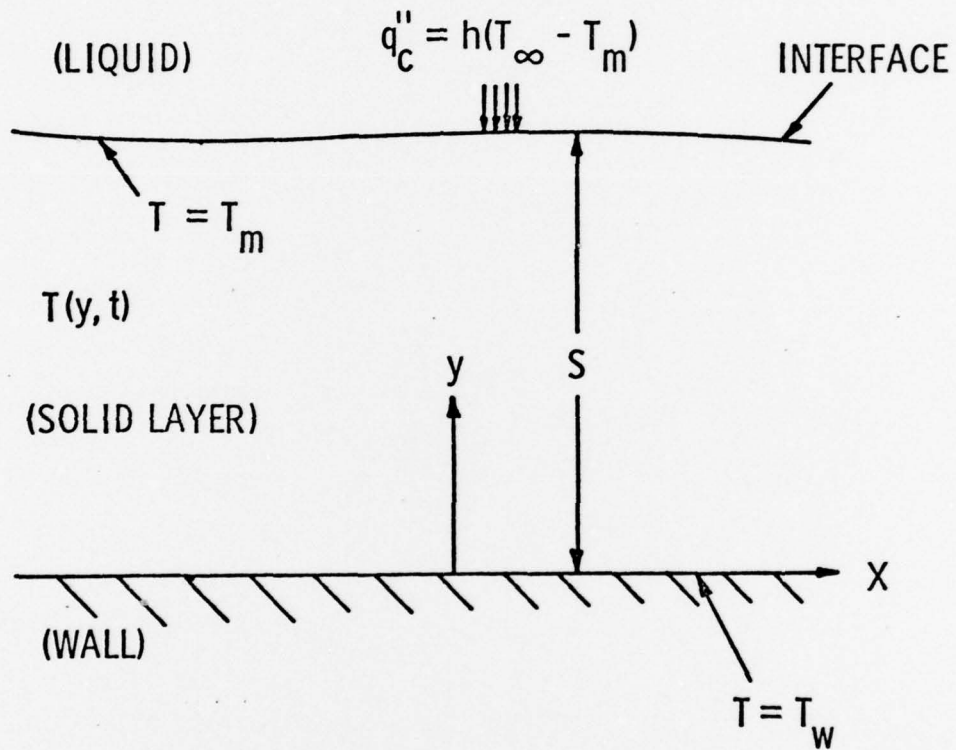


Figure 1 - Sketch Illustrating the Basic Arrangement of Solid Layer, Rigid Wall, and Liquid Freestream.

- h - local convective conductance based upon  $T_\infty$ , the liquid freestream temperature
- $q_c''$  - local convective heat flux at the solid-liquid interface
- S - solid layer thickness
- T - temperature in the solid layer
- $T_m$  - equilibrium fusion temperature of the substance
- $T_w$  - local wall temperature
- t - time coordinate measured from some convenient origin
- x - position coordinate measured parallel to the rigid wall
- y - position coordinate measured perpendicular to the wall

The wall is assumed to be either a plane wall or one in which the local radius of curvature is large with respect to the local solid layer thickness, S. This assumption is made because in the present study a Cartesian coordinate system is used, but the same basic type of analysis and procedure could be applied in either cylindrical or spherical coordinate systems. At the solid-liquid interface, ( $y=S$ ), the solid surface is subject to the convective heat flux from the warmer liquid which is of course a function of the local convective conductance, h, and the freestream temperature,  $T_\infty$ . At the wall, ( $y=0$ ), the layer is in direct contact with the solid wall which is assumed always to be at some temperature less than the fusion temperature, hence some solid is always present. The assumption of direct contact between solid and wall implies the absence of any contact resistance and therefore the temperature of the solid at  $y=0$  is equal to the wall temperature. It is important to note that in this analysis no assumptions will be made regarding the form of the time variation of the wall temperature,  $T_w$ , and the convective heat flux,  $q_c''$ . On the other hand both  $T_w$  and  $q_c''$  must be known as

functions of time before the problem solution can begin. Specification of the heat flux at the interface implies that the fluid dynamical problem for the region  $y > S$  is independent of the solid layer thickness. This can usually be justified as a reasonable assumption in external flow situations when  $S$  is small, but for internal flows the variation in solid thickness may have a significant effect on the fluid flow itself. In such a case the equations governing the flow in the region  $y > S$  are coupled at the solid-liquid interface to the equations governing the solid layer thickness. A more complete discussion of the assumptions made in this analysis is given immediately below.

### III. Basic Assumptions in Model Formulation

The following simplifying assumptions will apply throughout the remainder of this paper.

1. Heat transfer within the solid layer is primarily one-dimensional and in a direction normal to the solid wall. This assumption is completely justified when the solid layer thickness,  $S$ , is relatively small with respect to other characteristic dimensions of the problem. The validity of this assumption for thin solid layers is justified by the following order of magnitude analysis. Consider the two-dimensional, transient heat conduction equation,

$$\frac{1}{\alpha} \frac{\partial T}{\partial t} = \frac{\partial^2 T}{\partial y^2} + \frac{\partial^2 T}{\partial x^2} \quad , \quad \text{III-1}$$

where  $\alpha$  is the thermal diffusivity of the solid. Introduce the two characteristic length scales  $d$  and  $L$  where  $d$  is the scale factor for the coordinate measured perpendicular to the wall,  $y$ . For  $d$  to be a characteristic length in the transverse direction it must be of the same order of magnitude as the solid layer



thickness,  $S$ . Thus,

$$d \sim O(S).$$

$L$  is the scale corresponding to the coordinate measured parallel to the wall,  $x$ . The two-dimensional energy equation is nondimensionalized with the length scales  $d$  and  $L$  and the fusion temperature,  $T_m$ , yielding.

$$\frac{\partial T}{\partial t'} = \frac{\partial^2 T}{\partial Y^2} + \left(\frac{d}{L}\right)^2 \frac{\partial^2 T}{\partial X^2}, \quad \text{III-2}$$

where,

$$T = \frac{T}{T_m},$$

$$Y = \frac{y}{d},$$

$$X = \frac{x}{L}, \text{ and,}$$

$$t' = \frac{t\alpha}{d^2}.$$

The scaling factors  $d$ ,  $L$ , and  $T_m$  were chosen so that  $Y$ ,  $X$ , and  $T$  are all of unity order.

$$Y = \frac{y}{d} \sim O(1)$$

$$X = \frac{x}{L} \sim O(1)$$

$$T = \frac{T}{T_m} \sim O(1)$$

If the solid layer thickness is small in comparison to its extension in the  $x$  direction then,

$$\frac{d}{L} \sim O(\delta), \text{ where } \delta \ll 1.$$

The right hand side of the energy equation III-2 becomes, symbolically,

$$\frac{\partial^2 T}{\partial Y^2} + \left(\frac{d}{L}\right)^2 \frac{\partial^2 T}{\partial X^2} \sim \frac{1}{1^2} + \delta^2 \frac{1}{1^2} \sim 1 + \delta^2.$$

Therefore approximately,

$$\frac{\partial T}{\partial t} = \frac{\partial^2 T}{\partial Y^2} , \quad \text{II-3}$$

and the one dimensional assumption is seen to be justified for thin solid layers. Note, however, that the above argument breaks down near edges or discontinuities in the wall because the assumption

$$\frac{d}{L} \ll 1$$

is no longer justified in these regions.

2. The wall temperature,  $T_w$ , and the convective heat flux at the interface,  $q_c''$ , are not dependent upon the solid layer thickness.

The equation governing the temperature distribution in the solid layer is therefore uncoupled from the energy equation governing the wall temperature and the equations of fluid dynamics governing the liquid flow.

3. The material under consideration is a pure substance. The complexities which arise due to phase change temperature ranges and solid state phase transformations in multicomponent systems are not considered here. With respect to alloy systems, for example, Friedman (4) has approached the phase change problem successfully with a finite element technique, however, the present analysis will apply only to pure substances, homogenous in the solid phase.

4. All solid properties are temperature independent. This assumption will not severely affect the accuracy of the results in problems where temperature differences in the solid are not extreme, i.e. for cases in which there is a moderate degree of subcooling.



5. Thermodynamic equilibrium exists at the solid-liquid interface, in other words, the interface temperature is assumed equal to the fusion temperature at all times.

#### IV. Mathematical Formulation

For the assumptions stated above the temperature distribution in the solid layer is governed by the following equation,

$$\alpha \frac{\partial^2 T}{\partial y^2} = \frac{\partial T}{\partial t}, \quad 0 < y < S. \quad \text{IV-1}$$

The boundary conditions are obtained directly from Figure 1.

Initially,

$$t = 0: \quad T = T(y), \quad \text{IV-1a}$$

$$S = S_0. \quad \text{IV-1b}$$

At the wall,

$$y = 0: \quad T = T_w. \quad \text{IV-1c}$$

At the solid-liquid interface,

$$y = S: \quad T = T_m. \quad \text{IV-1d}$$

One other condition must be specified at the interface. This condition relates the energy fluxes at  $y = S$  to the rate of latent heat evolution due to phase change. In words: The rate of energy transport by convection to the interface from the flowing liquid plus the rate at which energy is evolved due to the latent heat of phase change is equal to the rate of energy transport away from the interface and into the solid layer by conduction, or,

$$\text{at } y = S: \quad q_c'' + \rho \lambda \frac{dS}{dt} = k \frac{\partial T}{\partial y}. \quad \text{IV-1e}$$

The symbols in equations IV-1 have the following meanings:

- $\alpha$  - thermal diffusivity of the solid
- $\rho$  - mass density of the solid
- $c$  - heat capacity of the solid
- $k$  - thermal conductivity of the solid
- $\ell$  - latent heat of phase change

Equations IV-1 completely define the present problem mathematically.

No general solution exists at this time for the system, IV-1.

The major difficulty with respect to analytical treatment arises from the interface boundary condition, IV-1e, as shown below.

In general, the temperature in the solid layer is both a function of position and time, thus,

$$T = T[y,t]$$

and

$$dT = \frac{\partial T}{\partial y} dy + \frac{\partial T}{\partial t} dt.$$

at  $y = S$ ,

$$T = T_m, \text{ and}$$

$$dT = \frac{\partial T}{\partial y} dy + \frac{\partial T}{\partial t} dt = 0 .$$

Upon rearrangement this becomes,

$$\left. \frac{dy}{dt} \right|_{y=S} = - \left( \frac{\frac{\partial T}{\partial t}}{\frac{\partial T}{\partial y}} \right)_{y=S} = \frac{dS}{dt} .$$

Substituting this result into condition IV-1e results in,

$$k \left. \frac{\partial T}{\partial y} \right|_{y=S} - q_c'' = - \rho \ell \left( \frac{\frac{\partial T}{\partial t}}{\frac{\partial T}{\partial y}} \right)_{y=S} .$$

The interface boundary condition, IV-1e, is therefore nonlinear and it is this nonlinearity which causes analytical difficulty.

V. Methods of Analysis

As mentioned earlier, exact analytical solutions are available for phase change problems only of the most fundamental variety. These particular solutions apply only for special forms of conditions IV-1a, b, c, and e. Consider, for example, the classical Stefan solution. This closed form solution applies to a semi-infinite region which initially consists of a single phase (liquid) at the fusion temperature. At zero time the boundary temperature,  $T_w$  is stepped down to some lower temperature thus initiating formation of the solid phase. The boundary temperature remains constant thereafter. In this instance the liquid phase is spatially isothermal at the fusion temperature and condition IV-1e simplifies to,

$$k \frac{\partial T}{\partial y} \Big|_{y=S} = \rho \ell \frac{dS}{dt} .$$

With this simplification and the assumption of constant wall temperature a similarity solution is possible with,

$$\eta = \frac{y}{2\sqrt{\alpha t}} \quad (\text{similarity variable}).$$

When this relation is substituted into system IV-1 an ordinary differential equation results which can be integrated to yield the temperature distribution in the solid and the interface position,

$$T - T_w = (T_m - T_w) \frac{\text{erf}\left(\frac{y}{2\sqrt{\alpha t}}\right)}{\text{erf}(b)} , \quad \text{V-1}$$

$$S = 2b\sqrt{\alpha t} , \quad \text{V-2}$$

where the constant,  $b$ , is given by,

$$be^{b^2} \operatorname{erf}(b) = \frac{c(T_m - T_w)}{2\sqrt{\pi}} \quad V-3$$

Obviously, the practical application of this solution is severely limited by the restrictive boundary conditions which were imposed in order to yield the closed form solution, V-1.

In contrast to the Stefan solution, I. G. Portnov (3) obtained a series solution to a slightly more general problem by Laplace transform methods. However, according to the paper of K. Stephan (5) the evaluation of even the first few coefficients in the series is very cumbersome.

In order to relax the restrictions imposed by an analytical solution, many investigations have employed approximate solution techniques, the most popular of which are the integral analyses. A brief description of the integral method is given below, however, a much more complete account may be found in Schlichting (6) and in Özisik (7).

The basic procedure used in most integral analyses in heat transfer and fluid dynamics is to first approximate the unknown temperature or velocity profile by some functional relationship, the form of which is chosen in order to satisfy the boundary conditions for the given problem. The governing equation (equation of motion or energy) is then integrated, using the approximate profile, with respect to one of the spatial variables. The resulting ordinary differential equation is then in terms of the second independent variable and may be solved by standard methods. The overall effect of the integral method then is the same as the effect of the similarity transformation in that the original partial differential equation is reduced to an ordinary differential equation.



In contrast to the similarity solutions the integral solution can only be an approximation because the assumed profile satisfies the original governing equation only at certain specific points within the given region, at the boundaries for example. It follows then, that the greater the number of boundary conditions satisfied by the assumed profile the more accurate the resulting integral solution. In many cases there is a choice as to which boundary conditions are to be used in developing the approximate profile. In this case the conditions should be chosen for the boundaries which are the most critical in a given situation so that the assumed profile will be especially accurate in these regions. In the phase change problem, for example, it is imperative that the interface heat balance condition, IV-1e, be used in forming the approximate profile. Integral techniques have been successfully applied to melting and solidification problems by T. R. Goodman (8), P. A. Libby and S. Chen (9), J. M. Savino and R. Siegel (10), and K. Stephan (5). All of the studies mentioned here report results which are usually well within the limits of accuracy normally required for engineering purposes. For instance, Stephan reports integral results which are in error by less than 2.5 percent when compared to presumably exact numerical solutions. Despite these promising results the applicability of integral techniques has thus far not been justified in more general phase change problems where the temperature profile within the solid may not be approximated well by a simple polynomial. Such situations may arise when the wall temperature and/or the heat flux are varied in an irregular manner. The integral technique is a powerful method of solution when applied to phase change problems but, more work must be done in order to establish the limitations involved

when using this type of approximate analysis.

Another approximate method which has been used successfully in phase change investigations involves the variational technique developed by Biot (11). This method was applied to the case of constant wall temperature solidification by C. Lapadula and W. K. Mueller (12). The results of their work are comparable in accuracy to the integral method used by Libby and Chen with the additional benefit that the solution is available in closed form. On the whole, however, variational techniques are not nearly as popular as integral methods and integral techniques therefore are responsible for the bulk of the approximate solutions.

The third major category of solution methods are the finite difference techniques. The principal advantage of numerical solution is, of course, the inherent immunity of these methods to nonlinearities, time varying boundary conditions, etc.. But even finite difference methods are adversely affected by the moving boundary characteristic of all phase change phenomena. In fixed nodal arrangements, the solid-liquid interface must move toward, reach, and pass-by each stationary temperature node so that when the interface is located between two nodes its exact position is unknown and therefore it must be located approximately by interpolation. A continuous account of the fusion front travel becomes then somewhat of a problem. The difference equations and interpolation formulae can become very complex, especially when solution in two space dimensions is considered, for example, see Springer and Olson (13). A unique nodal scheme for one-dimensional problems which eliminates the need for interpolation and yields a continuous, accurate account of the fusion front motion was suggested by Murray and Landis (14). In this nodal arrangement, the nodal mesh



changes continuously with fusion front travel so that the interface position is always coincident with a temperature node, thus there is no need for interpolation and the difference formulae are simplified considerably.

Numerical techniques provide a means of obtaining an accurate solution to the phase change problem outlined in Part II for realistic boundary conditions. Because it is a primary aim of this study to present a method of solution which is of a general nature, numerical methods will be applied here, namely, a finite difference technique similar to that used by Murray and Landis.

VI. Nondimensionalization and Asymptotic Solution

The following dimensionless groups are defined:

$$y^* = \frac{y}{S_0}, \text{ dimensionless space coordinate,}$$

$$t^* = \frac{t\alpha}{S_0^2}, \text{ dimensionless time coordinate (Fourier Modulus),}$$

$$\theta = \frac{T - T_w}{T_m - T_w}, \text{ dimensionless temperature,}$$

$$S^* = \frac{S}{S_0}, \text{ dimensionless solid layer thickness,}$$

where  $S_0$  denotes the solid layer thickness at zero time,  $t = t^* = 0$ .

Substituting these dimensionless variables into equations IV-1 results in the following nondimensional system.

$$0 < y^* < S^*: \quad \frac{\partial^2 \theta}{\partial y^{*2}} = \frac{1}{S_t} \frac{dS_t}{dt^*} [\theta - 1] + \frac{\partial \theta}{\partial t^*} \quad \text{VI-1}$$

$$t^* = 0: \quad \begin{cases} \theta = \theta(y^*), & \text{VI-1a} \\ S^* = 1. & \text{VI-1b} \end{cases}$$

$$y^* = 0: \quad \theta = 0. \quad \text{VI-1c}$$

$$y^* = S^*: \quad \left\{ \begin{array}{l} \theta = 1, \\ S_t \frac{\partial \theta}{\partial y^*} - q^* = \frac{dS^*}{dt^*} . \end{array} \right. \quad \begin{array}{l} \text{VI-1d} \\ \text{VI-1e} \end{array}$$

The new parameters resulting from the nondimensionalization are defined as,

$$q^* = \frac{q_c'' S_0}{\ell \rho \alpha}, \text{ dimensionless heat flux,}$$

$$S_t = \frac{c(T_m - T_w)}{\ell}, \text{ Stefan number.}$$

Both  $q^*$  and  $S_t$  are assumed to be time dependent in the general case.

The steady state thickness is obtained from equations VI-1 as follows. Under steady state conditions VI-1 reduces to,

$$\frac{\partial^2 \theta}{\partial y^{*2}} = 0. \quad \text{VI-2}$$

Using VI-1c and VI-1d in VI-2,

$$\theta_{ss} = \frac{y^*}{S_{ss}^*} \text{ (linear profile).} \quad \text{VI-3}$$

Substituting VI-3 into the interface boundary condition VI-1e results in,

$$\frac{S_{tss}}{S_{ss}^*} - q_{ss}^* = 0 \quad \text{or,}$$

$$S_{ss}^* = \frac{S_{tss}}{q_{ss}^*}, \quad \text{VI-4}$$

where  $q_{ss}^*$ ,  $S_{tss}$ , and  $S_{ss}^*$  are the values of  $q^*$ ,  $S_t$ , and  $S^*$  respectively under steady state conditions. When dimensional quantities are reintroduced, equation VI-4 is seen to be merely a statement of the equality of heat flux by conduction through the solid layer to the rate at which energy is convected to the interface from the liquid,

$$(q_c'')_{ss} = \frac{k(T_m - T_w)_{ss}}{S_{ss}} .$$

Probably one of the most important results of the normalization of equations IV-1 is the appearance of the parameter,  $S_t$  (termed "Stefan number"). The physical interpretation usually associated with  $S_t$  is obtained directly from the definition,

$$S_t = \frac{c(T_m - T_w)}{\ell} \sim \frac{\text{sensible heat}}{\text{latent heat}} .$$

Thus, the Stefan number is often interpreted as a measure of the relative effects of sensible and latent heat in the solid layer. It is shown by Lock (15) that in cases for which convection effects are small at the interface,

$$\frac{1}{S_t} \sim F_o \text{ (Fourier Modulus).}$$

Therefore small values of  $S_t$  imply large values of  $F_o$ , which in turn implies the approach toward steady state conditions within the solid layer (recall that a large Fourier modulus indicates that heat capacity effects are small with respect to heat conduction effects). To further illustrate the physical significance of this parameter, consider the case in which the Stefan number assumes a very small value, indicating small heat capacity effects in the solid, i.e.

$$S_t \ll 1, \text{ and } F_o \gg 1 .$$

If convection effects are also small and the wall temperature is constant, then, VI-1 reduces approximately to,

$$\frac{\partial^2 \theta}{\partial y^{*2}} \approx 0 . \tag{VI-5}$$

Thus, the temperature profile must be approximately linear,

$$\theta \approx \frac{y^*}{S^*} . \tag{VI-6}$$

Using this result in condition VI-1e yields,

$$\frac{dS^*}{dt^*} = \frac{S_t}{S^*} - q^* \quad \text{VI-7}$$

Equation VI-7 is an expression for  $S^*$  as a function of  $t^*$  in the case of constant wall temperature and very small Stefan number. Assuming further a constant value of heat flux ( $q^* = \text{constant}$ ) and interchanging independent and dependent variables results in,

$$t^* = \int_1^{S^*} \frac{\phi d\phi}{S_t - q^* \phi}, \quad \text{VI-8}$$

where  $\phi$  denotes a dummy variable of integration.

Integrating VI-8,

$$t^* = \frac{1-S^*}{q^*} + \frac{S_t}{q^{*2}} \log \left( \frac{1 - \frac{q^*}{S_t}}{1 - \frac{q^* S^*}{S_t}} \right). \quad \text{VI-9}$$

Equation VI-9 is a closed form expression for  $S^*$  as an implicit function of  $t^*$  for the limiting case of  $S_t \rightarrow 0$ . This solution is of practical interest because in many cases  $S_t$  is indeed very small and VI-9 can then be expected to give totally satisfactory results. Ice is one substance for which equation VI-9 often applies, for ice,  $\ell/c \approx 288^\circ\text{F}$ .

## VII. Finite Difference Solution

In Figure 2 the  $N$  temperature nodes are spaced evenly throughout the solid layer with the 1st and  $N$ th nodes located at the wall and at the solid-liquid interface respectively. In order to maintain this configuration as the interface moves, each temperature node (excepting the first) must have a non-zero velocity with respect to the wall at  $y=0$ . The principal purpose for introducing the nodal mesh, of course, is to allow the approximation of equations VI-1 by finite difference



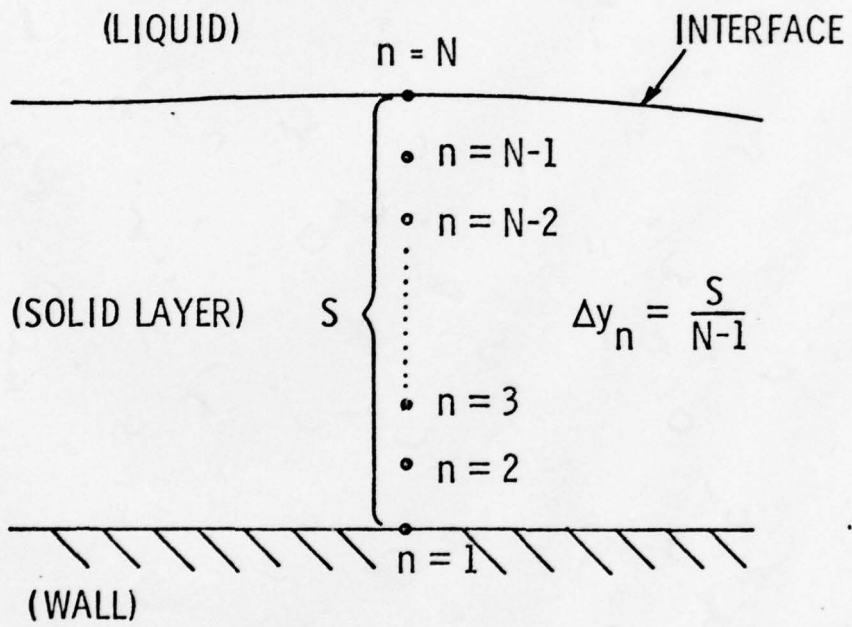


Figure 2 - Variable Nodal System.

formulae. With the above moving nodal arrangement, however, the time derivative, as it appears in equation VI-1, cannot be written in difference form for the reasons outlined below.

Writing the time derivative in the more explicit form,

$$\frac{\partial \theta}{\partial t^*} = \left( \frac{d\theta}{dt^*} \right)_{y^* = \text{constant}} \neq \frac{D\theta}{Dt^*} ,$$

emphasizes the important fundamental difference between the partial time derivative at a fixed point in space and the total time derivative of a moving point or particle. In order to express equation VI-1 in difference form, it must be written in terms of the total time derivative,  $\frac{D\theta}{Dt^*}$ , which is easily approximated by the nodal system in Figure 2.

Consider  $\theta$  to be a function of  $y^*$  and  $t^*$ ,

$$\theta = \theta[y^*, t^*] ,$$

$$d\theta = \frac{\partial \theta}{\partial t^*} dt^* + \frac{\partial \theta}{\partial y^*} dy^* ,$$

$$\frac{d\theta}{dt^*} = \frac{D\theta}{Dt^*} = \frac{\partial \theta}{\partial t^*} + \frac{dy^*}{dt^*} \frac{\partial \theta}{\partial y^*} ,$$

or,

$$\frac{\partial \theta}{\partial t^*} = \frac{D\theta}{Dt^*} - \frac{dy^*}{dt^*} \frac{\partial \theta}{\partial y^*} . \quad \text{VII-1}$$

Substituting into equation VI-1 results in,

$$\frac{D\theta}{Dt^*} = \frac{\partial^2 \theta}{\partial y^{*2}} - \frac{1}{S_t} \frac{dS_t}{dt^*} [\theta-1] + \frac{dy^*}{dt^*} \frac{\partial \theta}{\partial y^*} . \quad \text{VII-2}$$

Equation VII-2 is the one-dimensional, transient, heat conduction equation in a form applicable to points moving in the solid layer with velocity,  $\frac{dy^*}{dt^*}$ . The velocity of the  $n$ th node is related to the interface velocity by the following relationship,

$$\left. \frac{dy^*}{dt^*} \right|_n = \frac{y_n^*}{S^*} \frac{dS^*}{dt^*} , \quad \text{VII-3}$$



in which  $y_n^*$  denotes the position of the nth node. Substituting VII-3 into VII-2 and rewriting VII-2 for the nth nodal point yields.

$$\frac{D\theta_n}{Dt^*} = \frac{\partial^2 \theta}{\partial y^{*2}} \Big|_n - \frac{1}{S_t} \frac{dS_t}{dt^*} [\theta_n - 1] + \frac{y_n^*}{S^*} \frac{dS^*}{dt^*} \frac{\partial \theta}{\partial y^*} \Big|_n \quad \text{VII-4}$$

Equation VII-4 is substituted for equation VI-1 in the original set of non-dimensional equations which are now rewritten in a form applicable to the variable difference mesh in Figure 2.

$$\frac{D\theta_n}{Dt^*} = \frac{\partial^2 \theta}{\partial y^{*2}} \Big|_n - \frac{1}{S_t} \frac{dS_t}{dt^*} [\theta_n - 1] + \frac{y_n^*}{S^*} \frac{dS^*}{dt^*} \frac{\partial \theta}{\partial y^*} \Big|_n \quad \text{VII-5}$$

$$t^* = 0: \quad \begin{cases} \theta = \theta(y_n^*) & \text{VII-5a} \\ S^* = 1. & \text{VII-5b} \end{cases}$$

$$y_n^* = y_1^* = 0: \quad \theta = \theta_1 = 0. \quad \text{VII-5c}$$

$$y_n^* = y_N^* = S^*: \quad \begin{cases} \theta = \theta_N = 1, & \text{VII-5d} \\ S_t \frac{\partial \theta}{\partial y^*} \Big|_N - q^* = \frac{dS^*}{dt^*} & \text{VII-5e} \end{cases}$$

In the numerical solution of equations VII-5 all space derivatives were approximated with 3-point central difference formulas with the exception of the gradient in the interface equation which was approximated with a 3-point backward formula. The 3-point formula was chosen in favor of the simpler 2-point formula at the interface in order to minimize truncation error in this critical region. Both time derivatives of temperature and solid thickness were approximated by 2-point forward formulas. The detailed difference equations are listed in the appendix.

The explicit form of the difference equations simplifies the numerical solution of system VII-5 considerably, however, in an

explicit solution scheme the question of stability must be considered. According to Özisik (7) there is no general criterion for determining the stability limits for nonlinear problems. In most cases the stability bounds are determined by numerical experiment. For the present study, however, a somewhat different approach was taken. First, it was assumed that the general stability criterion for linear, parabolic, partial differential equations holds approximately in the nonlinear case (see Ames (16) ). Then as a second check on the stability of the solution a prediction-correction scheme was used. The corrector was applied to  $S^*$  at a given time step until successive corrections differed by less than some predetermined amount, or, if after four corrections the above step size control criterion still had not been satisfied the step size was halved and that iteration repeated. In this way a check on the stability and on the accuracy of the solution was achieved in one step. Both accuracy and stability are assured by the above procedure because in most cases accuracy strongly implies stability. A solution being carried out near the stability bound will exhibit a stable but slightly irregular behavior in advance of the point where the numerical algorithm becomes truly unstable. The above step size control procedure then, effectively detects impending instability by the slightly erratic behavior of the solution which immediately precedes it. This procedure has been used to obtain numerical results for a wide variety of initial and boundary conditions (including those in Part VIII) and to date no stability problems have been encountered.

#### VIII. Results and Conclusions

The numerical results in this section have been included to verify the validity and accuracy of the finite difference technique

developed in Part VII and to allow some basic observations to be made regarding the general behavior of the physical system outlined in Part II.

All curves were obtained with the moving nodal point network shown in Figure 2 using a total of ten temperature nodes (eight internal nodes). This mesh size was found to yield accurate results without an excessive amount of computational effort. For simplicity, each of the curves calculated (except for Figure 5) begins with a solid layer initially at steady state, i.e.,

$$\text{for } t^* < 0, S^* = 1, \frac{dS^*}{dt^*} = 0, \text{ and } S_{ti} = q_i^*$$

where  $S_{ti}$  and  $q_i^*$  denote the values of Stefan number and dimensionless heat flux respectively for times less than zero. At  $t^* = 0$ , either  $S_t$  or  $q^*$ , or both change from their initial value to some other value which may or may not remain constant with time, depending on the specified boundary conditions for the immediate problem.

The numerical solution can be compared to the exact analytical solution of Stefan for the special case of  $q^* = 0$ . This is a trivial example but it nevertheless provides an excellent means of checking on the performance of the finite difference calculation. It will be recalled that for the case of zero solid thickness initially and liquid at the fusion temperature the temperature distribution in the solid and the interface position at any time are given by equation V-1 and V-2 respectively.

$$T - T_w = (T_m - T_w) \frac{\text{erf} \left( \frac{y}{2\sqrt{\alpha\tau}} \right)}{\text{erf}(b)} \tag{V-1}$$

$$S = 2b\sqrt{\alpha\tau}, \tag{V-2}$$

where the constant  $b$ , is determined from,

$$b^2 e^{b^2} \text{erf}(b) = \frac{S_t}{\sqrt{\pi}} \tag{VIII-1}$$

The initial condition for the Stefan problem is unfortunately inconsistent with the requirement of the finite difference model that the solid layer always have a finite thickness. The difference in initial conditions is illustrated in Figures 3a, and 3b.

This discrepancy was accounted for in the numerical comparison by allowing the Stefan solution to proceed until the solid layer thickness,  $S$ , calculated by Equation V-2 was  $S_0$  in magnitude at which time the numerical solution was begun using the exact temperature profile given by Equation V-1 as an initial temperature distribution. The procedure is shown schematically in Figure 4.

In Figure 4,  $\tau$  is the time coordinate corresponding to the Stefan solution,  $\tau_0$  is the time required for the solid to build-up to a thickness  $S_0$  as given by Equation V-2, and  $t$  is the time coordinate for the finite difference calculation, the origin of which coincides with  $\tau = \tau_0$ . From Figure 4,

$$\tau = t + \tau_0 ,$$

so that equation V-2 becomes

$$S = 2b\sqrt{\alpha(t+\tau_0)} . \tag{VIII-2}$$

However, by definition,

$$S_0 = 2b\sqrt{\alpha\tau_0} ,$$

thus,

$$\tau_0 = \frac{S_0^2}{4b^2\alpha} .$$

Substituting this into Equation VIII-2 ,

$$S^2 = 4b^2 \alpha \left( t + \frac{S_0^2}{4b^2\alpha} \right) ,$$

$$\left( \frac{S}{S_0} \right)^2 = 4b^2 \frac{\alpha t}{S_0^2} + 1 ,$$



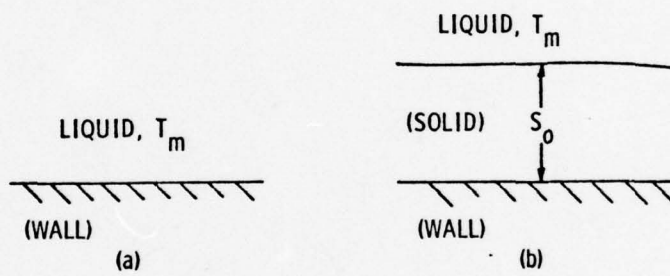


Figure 3 - Initial Condition for the Stefan Solution, No Solid Layer.

Initial Condition Specified in Part IV,  $S=S_0$  at  $t=0$ .

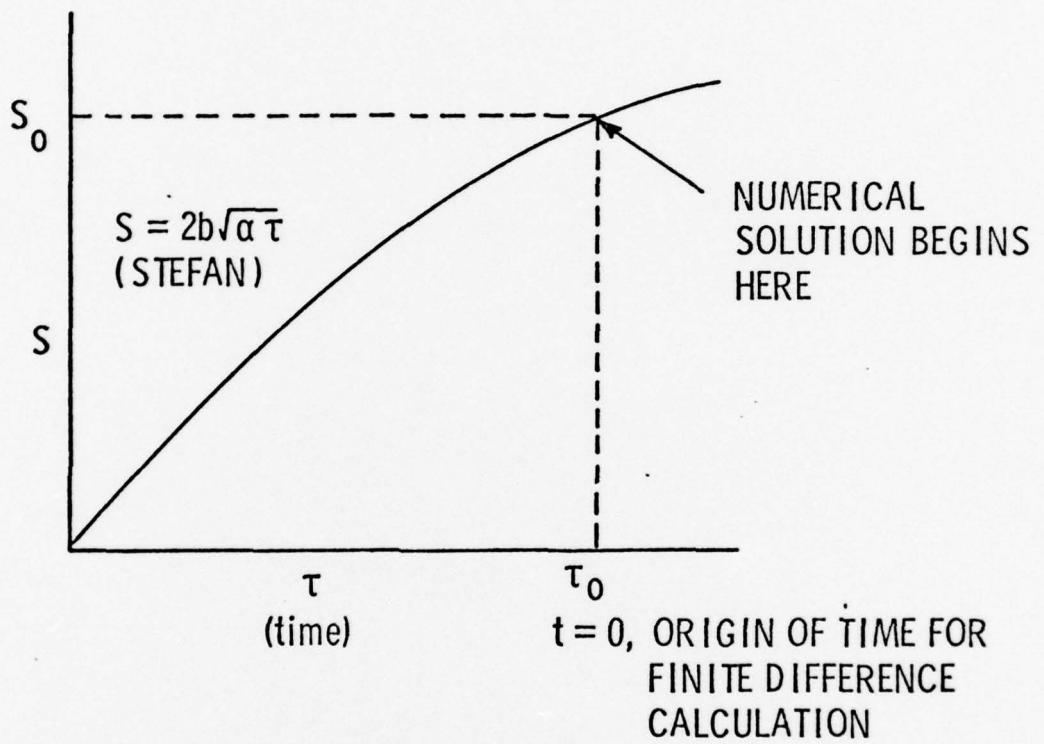


Figure 4 - Illustration of Method for Comparing the Exact and Numerical Solutions.

and,

$$S^{*2} = 4 b^2 t^* + 1 \quad . \quad \text{VIII-3}$$

Equation VIII-3 is the Stefan solution in terms of  $S^*$  and  $t^*$ , the pertinent variables in the numerical solution. Similarly, Equation V-1 becomes,

$$\theta = \frac{\operatorname{erf} \left( \frac{y^*}{2\sqrt{t^* + 1/4b^2}} \right)}{\operatorname{erf}(b)} \quad \text{VIII-4}$$

Equation VIII-4 was used to generate the initial temperature profile for the finite difference solution. For convenience the constant  $b$  was set equal to  $1/2$  so that Equation VIII-3 reduces to

$$S^* = \sqrt{t^* + 1} \quad , \quad \text{VIII-5}$$

with  $S_t = 0.5923$  from Equation VIII-1.

The results of this comparison are shown in Figure 5 in which the data points were plotted from the finite difference solution and the continuous curve is plotted from Equation VIII-5.

The discrepancy between the two solutions is so small that it cannot be easily seen from Figure 5. In actuality, the error in the finite difference results, in the range of time shown, is less than  $1/10$  of one percent based upon the "exact" results of Equation VIII-5. The same curve was extended to a  $t^*$  value of 10,000 to ascertain the effect of large values of  $S^*$  (large increments between temperature nodes) on the accuracy of the solution. At  $t^* = 10,000$ , at which time the solid thickness is 100 times its original thickness, the relative error in the numerical solution is still only about  $1/20$ th of one percent. From the results of this comparison it would seem safe to assume that the solution technique outlined in this paper does provide results which are highly reliable.

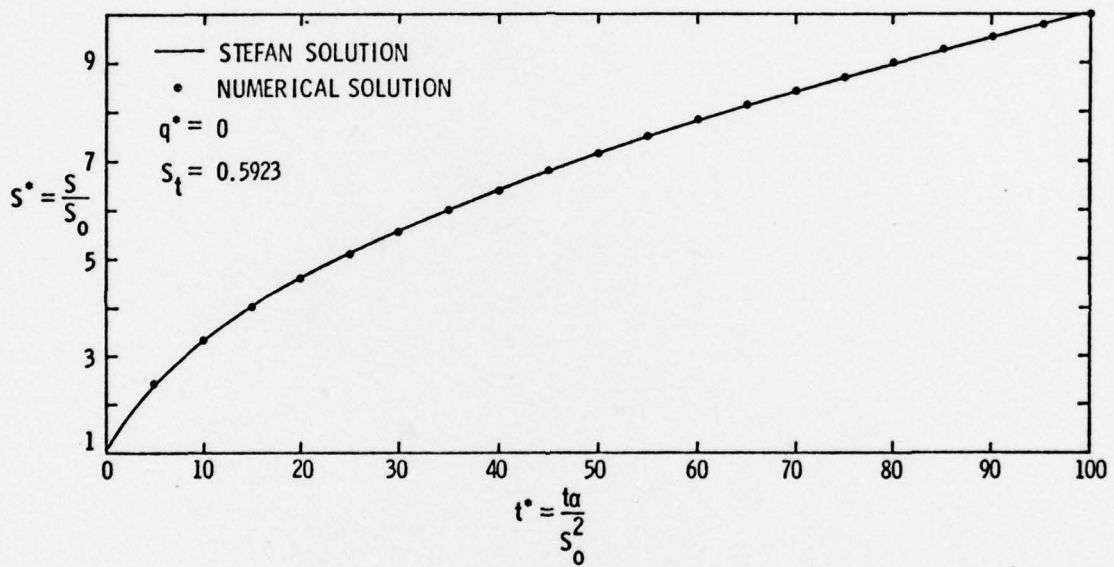


Figure 5 - Comparison of Exact (Stefan) and Numerical Solutions.



Figure 6 is a series of plots parametric in Stefan number verifying the effect of very small values of  $S_t$  on the solution for  $S^*$  (see part VI). For small values of  $S_t$  the temperature profile in the solid layer is virtually linear and the interface position is predicted quite well by Equation VI-9 denoted by the data points in Figure 6. However, as the Stefan number is raised, the heat capacity in the solid becomes more and more important and at  $S_t$  values approaching unity the predictions of equation VI-9, derived under the assumption of a linear profile, become poor approximations at best.

Also note that in each curve in Figure 6, Equation VI-9 overpredicts the magnitude of the interface velocity. The reason for this is easily shown by the dimensional form of the energy equation,

$$\frac{\partial^2 T}{\partial y^2} = \frac{1}{\alpha} \frac{\partial T}{\partial t} \quad \text{IV-1}$$

For growing solid layers, such as the ones in Figure 6, the right hand side of Equation IV-1 is always negative, indicating that the temperature profile is everywhere concave down, see Figure 7. The slope of the linear profile is seen to be greater than that of the actual profile at the interface, and therefore substitution of the linear relation VI-6 into condition IV-1e,

$$k \left. \frac{\partial T}{\partial y} \right|_{y=S} - q_c'' = \rho \ell \frac{dS}{dt} \quad \text{IV-1e}$$

will result in interface velocities in excess of those given by the finite difference solution. This qualitative result coincides with the results of Figure 6. Another very important point concerns the value of  $q^*$ , the heat flux parameter, used in the construction of the curves in Figure 6. If the value of  $q^*$  had been chosen close to unity very poor correlation would have resulted regardless of the value of

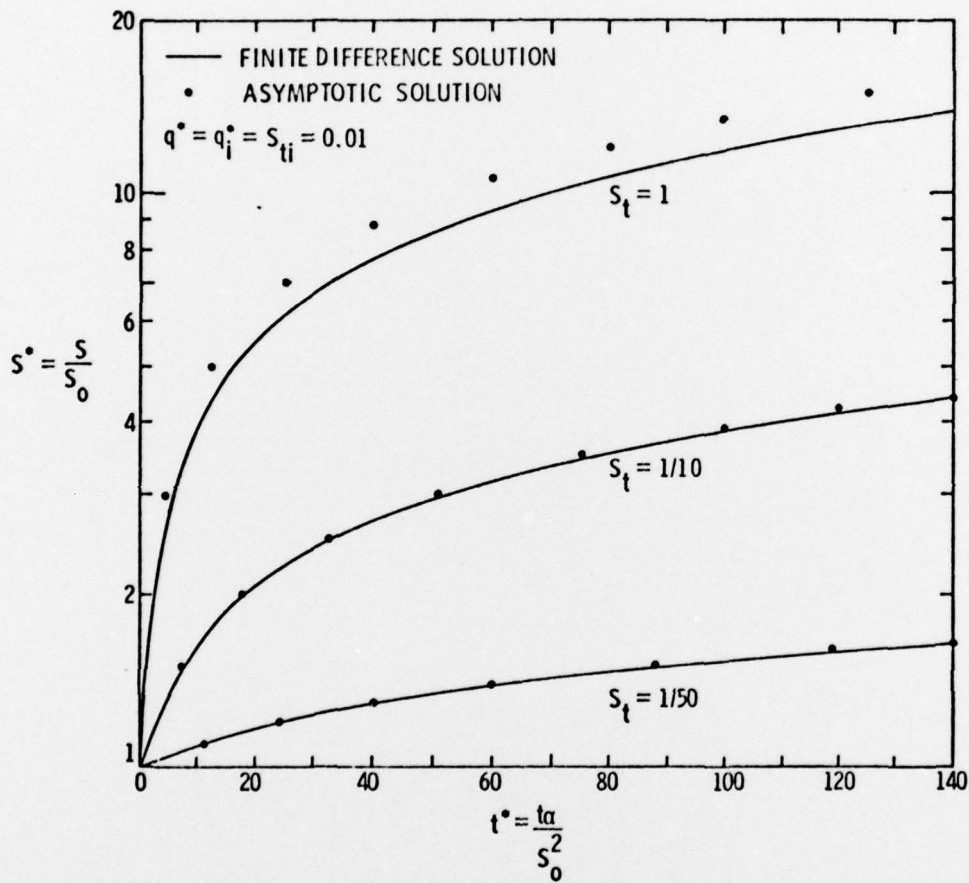


Figure 6 - Asymptotic Behavior for  $S_t \rightarrow 0$ .

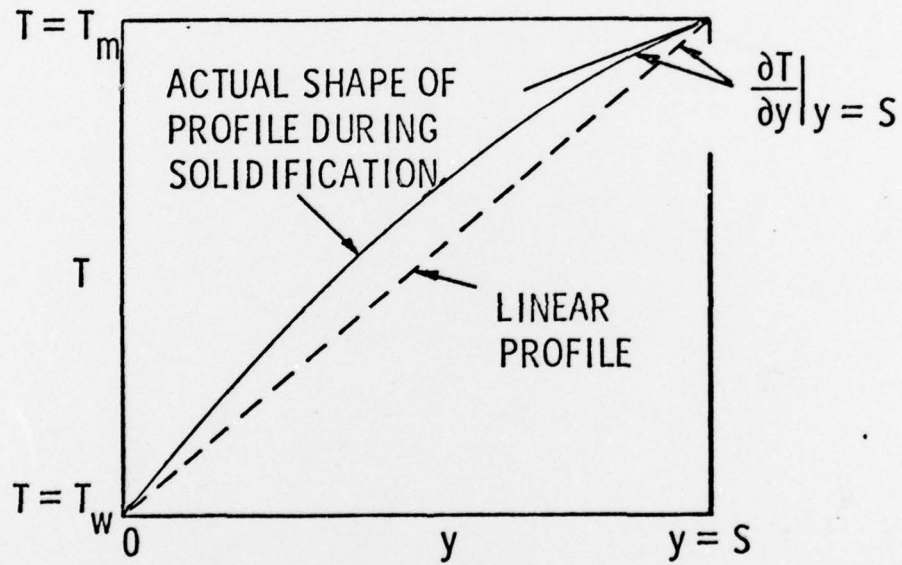


Figure 7 - Comparison of Temperature Gradients at the Interface, Actual Temperature Profile and Linear Approximation.

Stefan number used. The relationship between  $S_t$  and Fourier modulus cited in part VI has no meaning unless convection effects at the interface are sufficiently small. This important detail is implicit in the development of Equation VI-5, (see Reference (15)) and has been overlooked by at least one author (Reference (5) ).

Figures 8 through 11 were included in this section in order to give some indication of how the solid layer would behave when subjected to simple step changes in wall temperature or heat flux. One obvious conclusion to be made here is that for a melting layer, Figures 8 and 9, an increase in heat flux at the interface is much more effective in causing a response than an increase in wall temperature (for the same final value of  $S^*$ ). This effect becomes more and more pronounced as heat flux is increased and  $S_t$  is decreased.

In figure 11, the solid layer is growing (solidification) and the convective heat flux,  $q^*$ , is seen to have a substantial effect on the time required to reach steady state conditions. As the heat flux is diminished the curves approach the characteristic "square root" shape as in Figure 5. The general tendency in all the curves is toward short response times when the heat flux is large and the Stefan number is small. Figure 12 was included to show the variation in solid thickness for an arbitrary step-wise variation in convective heat flux which might occur during a load change in a device like the boiler-reactor referred to in Part I. In this particular case the wall temperature remained constant at the initial value but it could have just as easily been a step or continuously varying function of time. Figure 12 is therefore an illustration of the generality of the solution technique developed in Part VII.



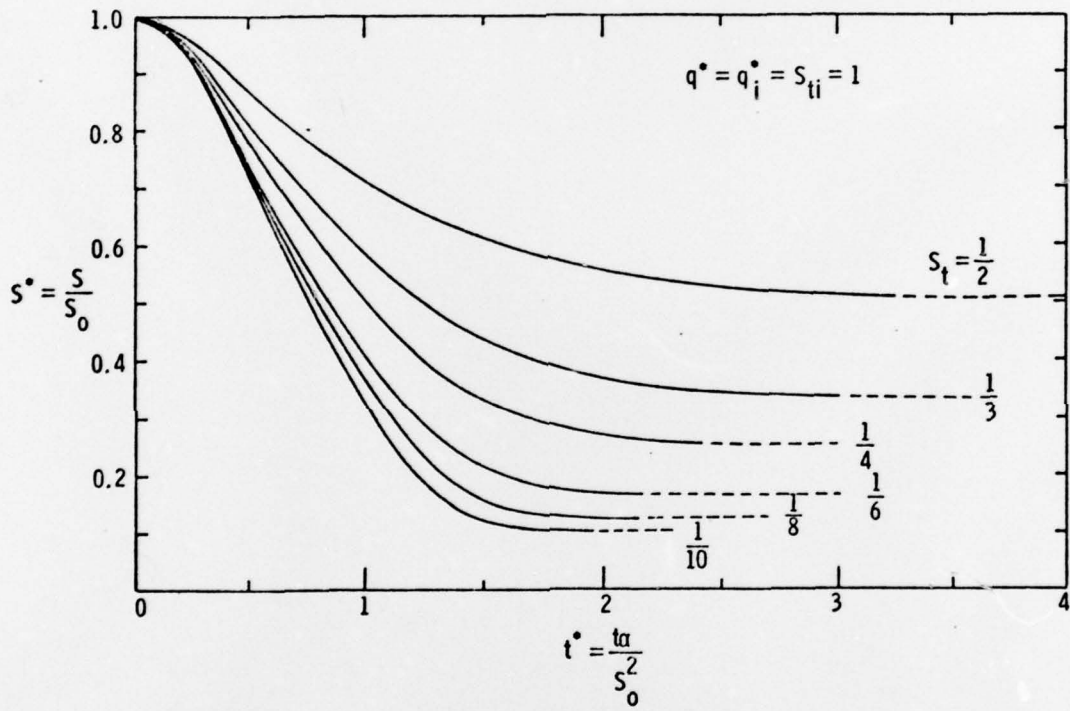


Figure 8 - Constant Heat Flux, Wall Temperature Stepped Up.

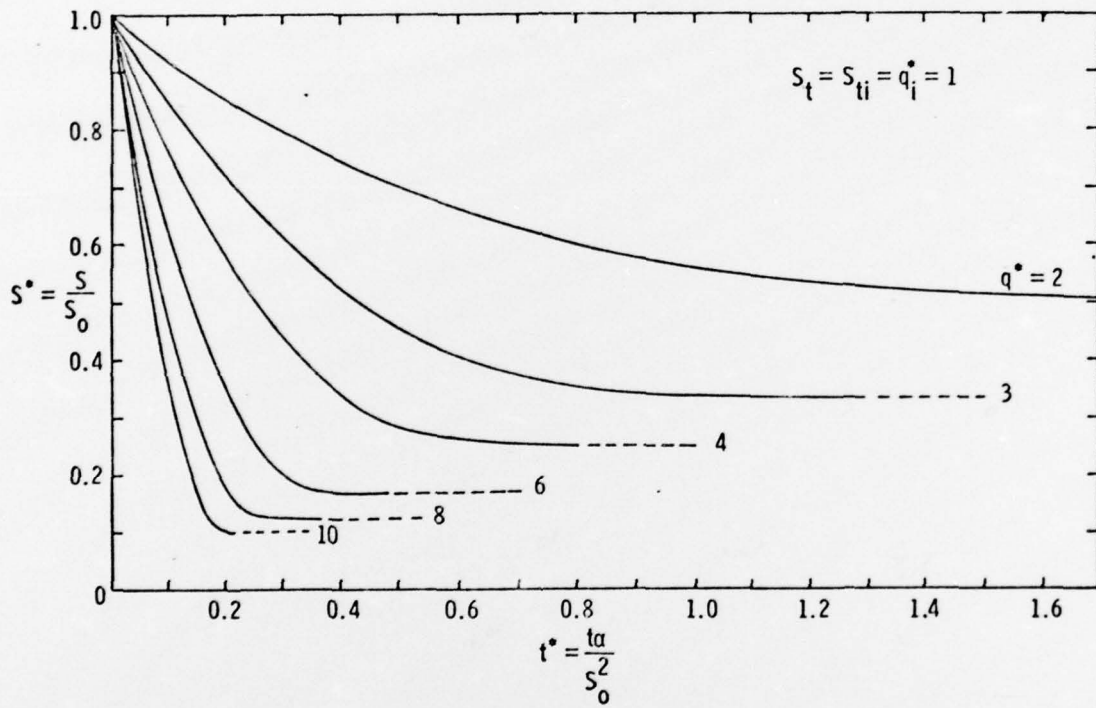


Figure 9 - Constant Wall Temperature, Heat Flux Stepped Up.

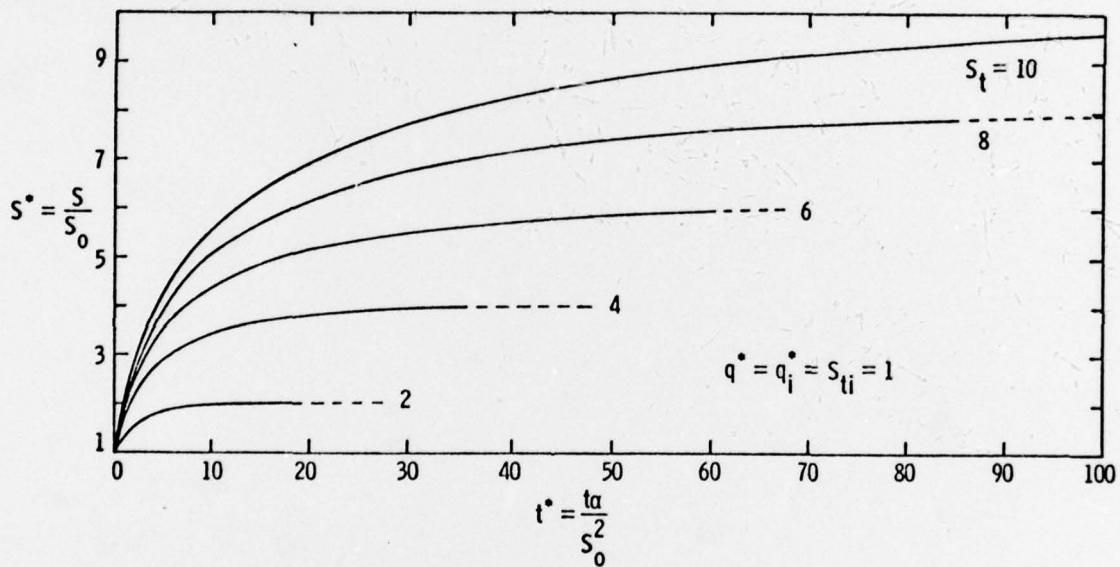


Figure 10 - Constant Heat Flux, Wall Temperature Stepped Down.

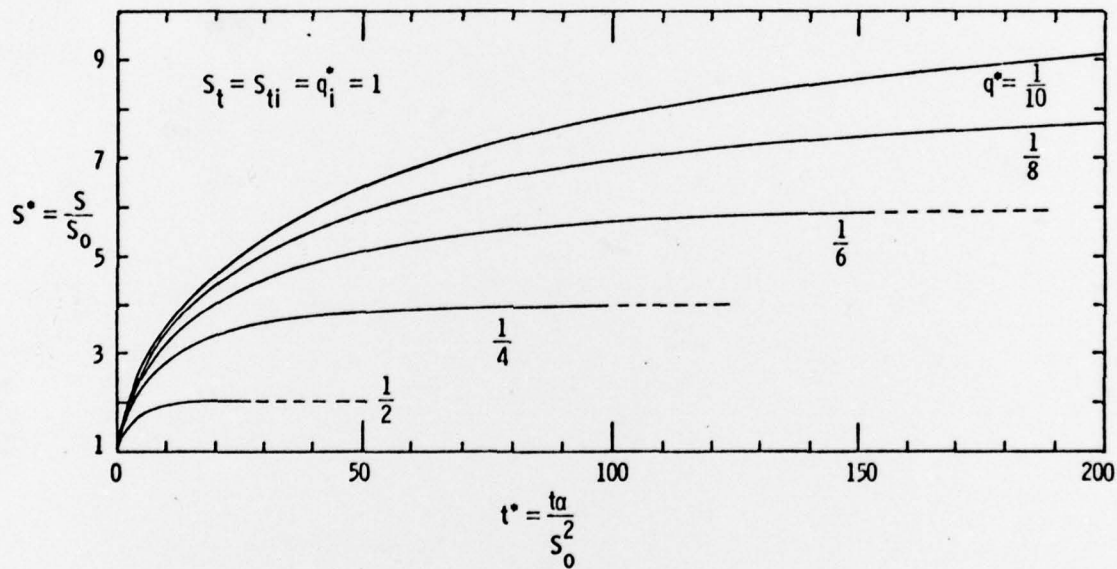


Figure 11 - Constant Wall Temperature, Heat Flux Stepped Down.



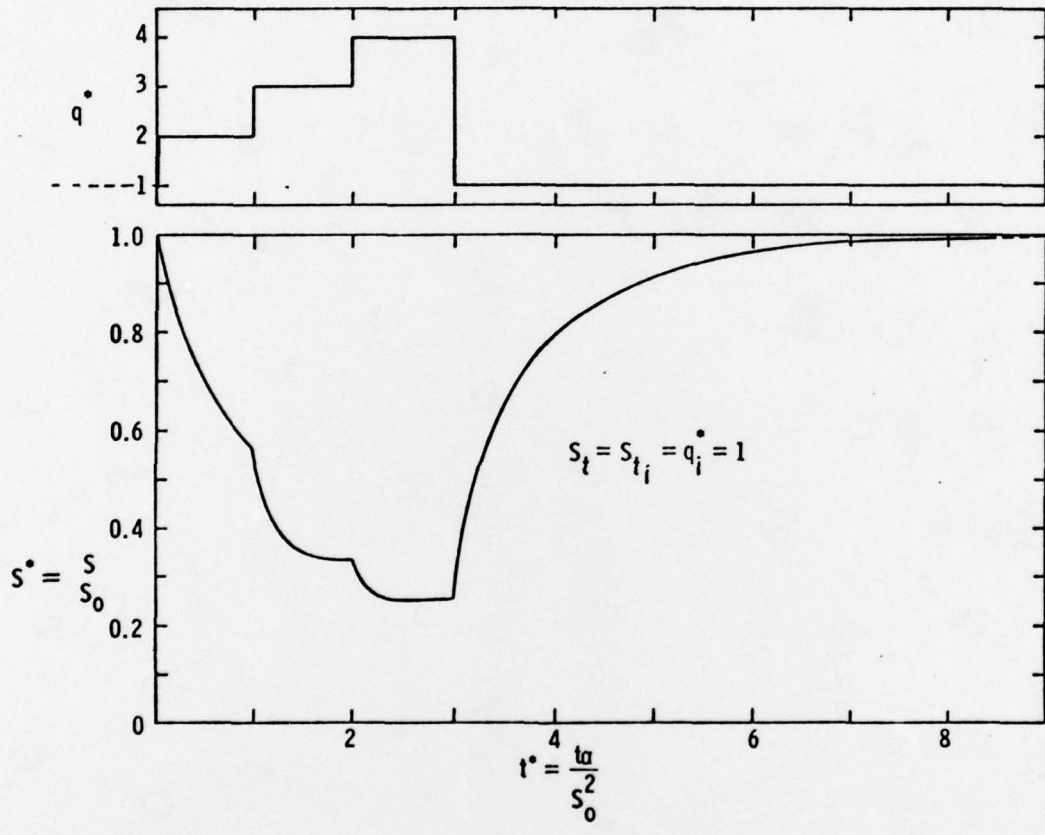


Figure 12 - Constant Wall Temperature, Step-Wise Heat Flux Variation.

In conclusion, the results presented here show relatively conclusively that the analysis developed in this paper for dealing with phase change-moving boundary type problems is capable of providing reliable, accurate data. This statement only holds true if the simplifying assumptions set forth in Part III can be applied to the physical problem without an excessive loss in realism. Probably the most conclusive way to show that the simplifying assumptions do not oversimplify the actual problem is by direct experiment. Such an experiment is at present in the developing stages and should eventually provide data to directly verify the analysis carried out here.

APPENDIX

## Difference Approximations

Equation VII-5:

$$\frac{\theta_n^{r+1} - \theta_n^r}{\Delta t^*} = \frac{(\theta_{n-1}^r + \theta_{n+1}^r - 2\theta_n^r)}{\Delta y^{*2}} - \frac{1}{S_t} \frac{dS_t}{dt^*} [\theta_n^r - 1] + \frac{y_n^*}{S^*r} \frac{dS^*}{dt^*} \frac{(\theta_{n+1}^r - \theta_{n-1}^r)}{2\Delta y^*} .$$

Equation VII-5e:

$$S_t \frac{(\theta_{N-2}^r - 4\theta_{N-1}^r + 3\theta_N^r)}{2\Delta y^*} - q^* = \frac{dS^*}{dt^*} = \frac{S^{*r+1} - S^{*r}}{\Delta t^*} .$$

In the above difference formulae "r" denotes the rth time step, "n" the nth nodal point, and "N" the interface node.

REFERENCES

1. H. S. Carslaw and J. C. Jaeger, Conduction of Heat in Solids, pp. 283 - 287, London (1959).
2. J. Stefan, "Über die Theorie der Eisbildung, insbesondere über die Eisbildung im Polarmeere," Annalen der Physik und Chemie, vol. 42, p. 269 (1891).
3. I. G. Portnov, "Exact Solution of Freezing Problem With Arbitrary Temperature Variation on the Fixed Boundary," Soviet Physics, Vol. 7, No. 3, p. 186 (1962).
4. E. Friedman, "An Iterative Procedure for Including Phase Change in Transient Conduction Programs and its Incorporation into the Finite Element Method," Submitted through, AIChE HT and EC Division for the 1977 National Heat Transfer Conference, Solidification and Melting Heat Transfer, p. 182.
5. K. Stephan, "The Influence of Heat Transfer on Melting and Solidification in Forced Flow," Int. J. Heat Mass Transfer, Vol. 12, pp. 199 - 214 (1969).
6. H. Schlichting, Boundary Layer Theorie, pp. 192 - 205, New York (1968).
7. M.N. Özisik, Boundary Value Problems of Heat Conduction, pp. 301 - 338, Scranton, PA. (1968).
8. T. R. Goodman, "The Heat Balance Integral and Its Application to Problems Involving a Change of Phase," Trans. A.S.M.E., Vol. 80, pp. 335 - 342 (1958).
9. P. A. Libby and S. Chen, "The Growth of a Deposited Layer on a Cold Surface," Int. J. Heat Mass Transfer, Vol. 8, pp. 395 - 402 (1965).
10. J. M. Savino and R. Siegel, "Experimental and Analytical Study of the Transient Solidification of a Warm Liquid Flowing Over a Chilled Flat Plate," NASA TN D-4015 (1967).
11. M. A. Biot, "New Methods in Heat Flow Analysis With Application to Flight Structures," J. Aeronaut. Sci., Vol. 24, pp. 857 - 873 (1957).
12. C. Lapadula and W. K. Mueller, "Heat Conduction With Solidification and a Convective Boundary Condition at the Freezing Front," Int. J. Heat Mass Transfer, Vol. 9, pp. 702 - 704 (1966).
13. G. S. Springer and D. R. Olson, "Method of Solution of Axisymmetric Solidification and Melting Problems," Contributed by the Heat Transfer Division for presentation at the Winter Annual Meeting, Nov. 25 - 30, 1962, of the ASME.



References (Continued)

14. W. D. Murray and F. Landis, "Numerical and Machine Solutions of Transient Heat Conduction Problems Involving Melting or Freezing," J. of Heat Transfer, The ASME, Series C, Vol. 81, pp. 106 - 112 (1959).
15. G. S. Lock, "The Growth and Decay of Ice," Int. Heat Transfer Conference, 5th Proc., Tokyo, Japan, Sept. 3 - 7, 1974, Vol. 6, Paper TL2, pp. 12 - 27 (1974).
16. W. F. Ames, Nonlinear Partial Differential Equations in Engineering, pp. 323 - 324, New York (1965).

Distribution List -- TM 78-175

NAVSEA, Mr. M. F. Murphy, SEA-0331C, Copy No. 1  
NAVSEA, Mr. J. W. Murrin, SEA-0331, Copy No. 2  
NAVSEA, Library, Code SEA-09G32, Copies No. 3 and 4  
NUSC, Mr. T. J. Black, Copy No. 5  
DDC, Copies No. 6 through 17